Intense dynamic bullets in a periodic lattice

P. Panagiotopoulos,[1,*] **A. Couairon,**[2] **N. K. Efremidis,**[3]
D. G. Papazoglou,[1,4] **and S. Tzortzakis**[1]

[1]*Institute of Electronic Structure and Laser, Foundation for Research and Technology Hellas, P.O. Box 1527, 71110, Heraklion, Greece*
[2]*Centre de Physique Théorique, École Polytechnique, CNRS, F-91128 Palaiseau, France*
[3]*Applied Mathematics Department, University of Crete, P.O. Box 2208, 71003, Heraklion, Greece*
[4]*Materials Science and Technology Department, University of Crete, P.O. Box 2208, 71003, Heraklion, Greece*

[*]*parisps@iesl.forth.gr*

Abstract: Femtosecond filamentation inside a periodic lattice in air is numerically shown to form intense dynamic bullets. The long propagation distance of the bullet structure is primarily attributed to the effect of the lattice that regulates the competition between linear and nonlinear spatiotemporal effects in the region of normal dispersion.

OCIS codes: (190.7110) Ultrafast nonlinear optics; (190.5940) Self-action effects; (320.0320) Ultrafast optics; (320.7110) Ultrafast nonlinear optics.

References and links

1. B. A. Malomed, D. Mihalache, F. Wise, and L. Torner, "Spatiotemporal optical solitons," J. Opt. B: Quantum Semiclassical Opt. **7**, R53 (2005).
2. Y. Silberberg, "Collapse of optical pulses," Opt. Lett. **15**, 1282–1284 (1990).
3. P. L. Kelley, "Self-focusing of optical beams," Phys. Rev. Lett. **15**, 1005–1008 (1965).
4. M. A. Porras, A. Parola, D. Faccio, A. Couairon, and P. Di Trapani, "Light-filament dynamics and the spatiotemporal instability of the Townes profile," Phys. Rev. A **76**, 011803R (2007).
5. G. Fibich and B. Ilan, "Optical light bullets in a pure Kerr medium," Opt. Lett. **29**, 887–889 (2004).
6. D. Mihalache, D. Mazilu, L.-C. Crasovan, I. Towers, A. V. Buryak, B. A. Malomed, L. Torner, J. P. Torres, and F. Lederer, "Stable spinning optical solitons in three dimensions," Phys. Rev. Lett. **88**, 073902 (2002).
7. D. E. Edmundson and R. H. Enns, "Robust bistable light bullets," Opt. Lett. **17**, 586–588 (1992).
8. S. K. Turitsyn, "Spatial dispersion of nonlinearity and stability of multidimensional solitons," Theor. Math. Phys. **64**, 226–232 (1985).
9. A. Couairon, "Light bullets from femtosecond filamentation," Eur. Phys. J. D **27**, 159-167 (2003).
10. A. B. Aceves, C. De Angelis, A. M. Rubenchik, and S. K. Turitsyn, "Multidimensional solitons in fiber arrays," Opt. Lett. **19**, 329-331 (1994).
11. B. B. Baizakov, B. A. Malomed, and M. Salerno, "Multidimensional solitons in a low-dimensional periodic potential," Phys. Rev. A **70**, 053613 (2004).
12. D. Mihalache, D. Mazilu, F. Lederer, Y. V. Kartashov, L.-C. Crasovan, and L. Torner, "Stable three-dimensional spatiotemporal solitons in a two-dimensional photonic lattice," Phys. Rev. E **70**, 055603 (2004).
13. D. Mihalache, D. Mazilu, F. Lederer, B. A. Malomed, Y. V. Kartashov, L.-C. Crasovan, and L. Torner, "Stable spatiotemporal solitons in Bessel optical lattices," Phys. Rev. Lett. **95**, 023902 (2005).
14. A. A. Sukhorukov and Y. S. Kivshar, "Slow-light optical bullets in arrays of nonlinear Bragg-grating waveguides," Phys. Rev. Lett. **97**, 233901 (2006).
15. X. Liu, L. J. Qian, and F. Wise, "Generation of optical spatiotemporal solitons," Phys. Rev. Lett. **82**, 4631 (1999).
16. P. Di Trapani, G. Valiulis, A. Piskarskas, O. Jedrkiewicz, J. Trull, C. Conti, and S. Trillo, "Spontaneously generated X-shaped light bullets," Phys. Rev. Lett. **91**, 093904 (2003).
17. A. Chong, W. H. Renninger, D. N. Christodoulides, and F. Wise, "AiryBessel wave packets as versatile linear light bullets," Nature Photon. **4**, 103–106 (2010).

#142489 - $15.00 USD Received 16 Feb 2011; revised 21 Mar 2011; accepted 29 Mar 2011; published 9 May 2011

18. D. Abdollahpour, S. Suntsov, D. G. Papazoglou, and S. Tzortzakis, "Spatiotemporal airy light bullets in the linear and nonlinear regimes," Phys. Rev. Lett. **105**, 253901 (2010).
19. N. K. Efremidis, K. Hizanidis, B. A. Malomed, and P. Di Trapani, "Three-Dimensional Vortex Solitons in Self-Defocusing Media," Phys. Rev. Lett. **98**, 113901 (2007).
20. J. M. Manceau, A. Averchi, F. Bonaretti, D. Faccio, P. Di Trapani, A. Couairon, and S. Tzortzakis, "Terahertz pulse emission optimization from tailored femtosecond laser pulse filamentation in air," Opt. Lett. **34**, 2165–2167 (2009).
21. S. Tzortzakis, G. Mechain, G. Patalano, M. Franco, B. Prade, and A. Mysyrowicz, "Concatenation of plasma filaments created in air by femtosecond infrared laser pulses," Appl. Phys. B **76**, 609–612 (2003).
22. A. Couairon and A. Mysyrowicz, "Femtosecond filamentation in transparent media," Phys. Rep. **441**, 47–189 (2007).
23. H. S. Chakraborty, M.B. Gaarde, and A. Couairon, "Single attosecond pulses from high harmonics driven by self-compressed filaments," Opt. Lett. **31**, 3662–3664 (2006).
24. P. Panagiotopoulos, N. K. Efremidis, D. G. Papazoglou, A. Couairon, and S. Tzortzakis, "Tailoring the filamentation of intense femtosecond laser pulses with periodic lattices," Phys. Rev. A **82**, 061803 (2010).
25. S. Suntsov, D. Abdollahpour, D. G. Papazoglou, and S. Tzortzakis, "Femtosecond laser induced plasma diffraction gratings in air as photonic devices for high intensity laser applications," Appl. Phys. Lett. **94**, 251104 (2009).
26. X. Yang, J. Wu, Y. Peng, Y. Tong, P. Lu, L. Ding, Z. Xu, and H. Zeng, "Plasma waveguide array induced by filament interaction," Opt. Lett. **34**, 3806–3808 (2009).
27. M. Leibscher, I. Sh. Averbukh, and H. Rabitz, "Molecular Alignment by Trains of Short Laser Pulses," Phys. Rev. Lett. **90**, 213001 (2003).
28. A. Szameit, D. Blmer, J. Burghoff, T. Schreiber, T. Pertsch, S. Nolte, A. Tünnermann, and F. Lederer, "Discrete nonlinear localization in femtosecond laser written waveguides in fused silica," Opt. Express **13**, 10552–10557 (2005).
29. G. G. Luther, J. V. Moloney, A. C. Newell, and E. M. Wright, "Self-focusing threshold in normally dispersive media," Opt. Lett. **19**, 862–864 (1994).
30. A. Couairon, E. Gaiauskas, D. Faccio, A. Dubietis, and P. Di Trapani, "Nonlinear X-wave formation by femtosecond filamentation in Kerr media," Phys. Rev. E **73**, 016608 (2006).

1. Introduction

One of the major goals in the study of nonlinear wave dynamics in optics is the generation of waves that propagate in the form of localized wavepackets in all the transverse dimensions of space, as well as in time i.e, nondiffracting and nondispersing [1]. Localization is typically achieved by nonlinearity that competes with the natural spreading of the wave in space and time. In a seminal paper, Silberberg proposed for the first time that Kerr nonlinearity can compensate for anomalous dispersion as well as diffraction leading to the formation of (3+1)D spatiotemporal solitons or light bullets [2]. Although the Silberberg light bullets are intrinsically unstable [3, 4], the possibility to stabilize the soliton dynamics by means of different effects attracted a lot of attention. Among the candidates, higher order dispersion [5], competing higher order [6] or saturating [7] nonlinearities, materials with nonlocal nonlinear response [8] as well as filamentation [9] were investigated. A different approach was suggested to stabilize discrete light bullets by means of periodic waveguide configurations [10]. Similar approaches have also been carried out in the continuous limit both in periodic two-dimensional lattices [11, 12] as well as in radially symmetric lattices [13]. Arrays of waveguides with Bragg gratings [14] have also been considered. Experimentally, 2D spatiotemporal solitons have been demonstrated in quadratic media [15]. Different types of spatiotemporal localized structures such as X-waves [16], Bessel-Airy linear bullets [17] and Airy-Airy-Airy nonlinear bullets [18] have been experimentally observed, whereas three-dimensional vortices [19] have been predicted. The main limiting factors in the experimental realization of light bullets are the anomalous dispersion and the slow time response of nonlinear media that mathematically support stable bullets. The availability of intense ultra-short light bullets in normally dispersive media would however offer ultimate control over a high power wavepacket, which could be used in various materials and have applications in fields like THz generation [20], telecommunications, optical metrology and sensing, long-range femtosecond filamentation [21] and attosecond pulse

#142489 - $15.00 USD Received 16 Feb 2011; revised 21 Mar 2011; accepted 29 Mar 2011; published 9 May 2011

generation [22,23]. In a recent work, we showed that filamentation of intense femtosecond laser pulses can be controlled with respect to its spatial properties by using optical lattices [24].

In this work, we exploit the filament dynamics in the presence of a lattice in both the spatial and the temporal domain. We find from numerical simulations that it is possible to generate spatiotemporal structures supporting intense laser propagation in normally dispersive air at a wavelength of 800 nm and remaining almost invariant (in space, time and maximum intensity) for over 90 cm in a lattice. We call these structures *intense dynamic bullets* (IDB) to distinguish them from perfectly stationary light bullets or solitons. The lattice is essential in the formation of the IDB. The role of each physical mechanism in the formation of the IDB is also analyzed.

2. Method

The lattice consists of concentric rings that describe a perturbation of the refractive index. These perturbations can be realized using different approaches for various transparent media. For example plasma can be used in the case of gases. One dimensional plasma lattices have recently been generated in air by interference of intense IR light beams for periodicities ranging from $\sim$500 nm [25] to 100 μm [26], and electron densities higher than 10^{18} cm^{-3}. The generation of cylindrically symmetric lattices is demanding but feasible since their Fourier transform is simply a sum of zero order Bessel functions. Note that the effect of such lattices on intense pulse propagation has not been explored yet. Thus, in principle, illumination of an amplitude mask allows the generation of intense concentric rings in the Rayleigh range of a long Fourier transforming lens. Furthermore, one could consider the use of positive or negative Δn lattices exploiting the molecular alignment of air molecules (or other gases). In the latter case the laser intensities needed are even lower than the ones needed for ionization and one can use pulse trains to further enhance the alignment [27] and consequently the strength of the lattice. Finally, in the case of filamentation in transparent solids, like glasses, one can use permanently written lattices in the bulk of the glass [28].

In our case, the cylindrically symmetric refractive index modulation is given by $n_{\rm cyl}(r) = n_0 + \Delta n$, for $\Delta n = \Delta n_0 \sum_{m=0} f(r - r_m)$. $f(r) = \exp[-(r/w)^{2p}]$ is the function describing the refractive index distribution of each ring, in our case a super-Gaussian of order $p = 8$ with width $w = 100\,\mu$m. The position of each ring is defined by $r_m \equiv [m + 1/2]\Lambda$. The period of the lattice is $\Lambda = 350\,\mu$m and the refractive index modulation is $\Delta n_0 = -3 \times 10^{-7}$. Assuming that plasma is used to generate such a modulation, this corresponds to a moderate plasma density of 10^{15} cm^{-3}. The laser pulse used in the simulations has a Gaussian spatiotemporal profile with a duration of 35 fs at FWHM and 500 μm beam width (1/e^2 radius). The 150 μJ pulse is lauched in the center cylinder of the refractive index modulation as it is shown in Fig. 1.

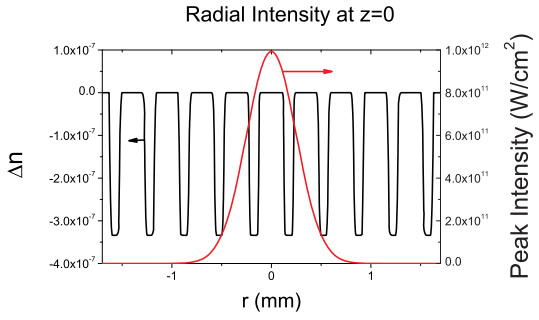

Fig. 1. (Color Online) Input radial intensity distribution superimposed on the lattice potential.

#142489 - $15.00 USD Received 16 Feb 2011; revised 21 Mar 2011; accepted 29 Mar 2011; published 9 May 2011

3. Numerical model

Our model relies on a nonlinear propagation equation along the z direction for the frequency components $\hat{E}(r,z,\omega)$ of the envelope $E(r,z,t)$ of the laser pulse coupled with an evolution equation for the electron density $\rho(r,z,t)$ generated by the intense pulse [22]:

$$\frac{\partial \hat{E}}{\partial z} = i\left[\frac{\Delta_\perp}{2\mathscr{K}_\omega} + D(\omega) + k_0\Delta n\right]\hat{E} + i\frac{\omega}{2c}\frac{\hat{P}_{NL}}{\varepsilon_0} \tag{1a}$$

$$\frac{\hat{P}_{\rm NL}}{\varepsilon_0} = 2n_0 n_2 \widehat{|E|^2 E} - \frac{\omega_0^2}{\omega^2}\widehat{\frac{\rho}{\rho_c}E} - \frac{c\beta_K}{\omega}\widehat{|E|^{2K-2}E} \tag{1b}$$

$$\frac{\partial \rho}{\partial t} = \sigma_K |E|^{2K}\rho_{\rm nt} \tag{1c}$$

The first term on the right hand side (rhs) of Eq. (1a) describes diffraction and space-time focusing through the operator $\mathscr{K}_\omega \equiv k_0 + k_0'\delta\omega$, $\delta\omega \equiv (\omega - \omega_0)$, $k_0 \equiv k(\omega_0)$. $k(\omega) \equiv \sum_m k_0^{(m)}(\delta\omega)^m/m!$ denotes the dispersion relation in air and $k_0^{(n)} = \frac{\partial^n k}{\partial\omega^n}|_{\omega_0}$ denote the dispersive coefficients corresponding to the frequency ω_0 of the carrier wave. Dispersion and the effect of the lattice are described by $D(\omega) \equiv k(\omega) - \mathscr{K}_\omega$ and Δn, respectively. The nonlinear polarization $\hat{P}_{\rm NL}(r,z,\omega)$ [Eq. (1b)] accounts for the optical Kerr effect, plasma defocusing, and multiphoton absorption (MPA), first calculated in the temporal domain and transformed into spectral components of $\hat{P}_{\rm NL}$. Pulse self-steepening is given by the explicit frequency dependence $\omega \equiv \omega_0 + \delta\omega$ in Eq. (1a). In some simulations discussed below and referred to as "Shock term off", its effect was switched off by setting $\omega = \omega_0$ in the explicit frequency dependence of the nonlinear polarization in Eqs. (1a) and (1b). The gas filling the gap of the lattice is air with nonlinear index $n_2 = 3.2\times10^{-19}$ cm^2/W, multiphoton ionization and absorption cross sections $\sigma_K = 3.4\times10^{-96}$ s^{-1}cm^{16}W^{-8} and $\beta_K = K\hbar\omega_0\rho_{\rm nt}\sigma_K$ for $K = 8$ photons. The density of neutral oxygen molecules is $\rho_{\rm nt} = 0.5\times10^{19}$ cm^{-3} and the critical plasma density is $\rho_c \simeq 1.7\times10^{21}$ cm^{-3}.

From Marburger's formula $P_{cr} = \frac{3.77\lambda^2}{8\pi n_0 n_2}$, the critical power for collapse of a Gaussian beam is $P_{cr} \sim 3$ GW. In the following we consider pulses with peak power of 1.25 P_{cr} and we stress that the critical power is only used as a reference indicating that a beam with the same input power would collapse in a pure Kerr medium. Due to the weak dispersion in air ($k'' \sim 0.2$ fs^2/cm), self-focusing prevails for input powers only a few percent above P_{cr} [29].

4. Simulation results and discussion

Figure 2 (Media 1) depicts the spatiotemporal reshaping of the laser pulse as it propagates in air without (top row) or with (bottom row) the lattice. In the case of standard filamentation in air, the intense pulse initially shrinks both in space and time due to the Kerr nonlinearity. At the nonlinear focus ($z \sim 130$ cm), the pulse becomes sufficiently intense to generate an underdense plasma which defocuses the pulse trailing part while nonlinear effects including the Kerr effect and multiphoton absorption compete to sustain propagation of the leading part in the form of a filament (130 cm $< z <$ 150 cm). Beyond the filamentation stage $z >$ 150 cm, the pulse finally widens due to diffraction and dispersion. Such behavior is typical for pulses undergoing filamentation and is accompanied by high nonlinear losses [22].

Propagation of the same intense pulse inside the lattice is significantly different: during the initial self-focusing stage, the beam does not shrink as much as it does without the lattice. After the initial self-focusing stage, the spatiotemporal dynamics reaches a quasi-equilibrium. The intensity profile of the resulting IDB remains almost stationary in both space and time for about 1 m, i.e a factor of 5 larger than the filamentation distance in air for the same input pulse. The

#142489 - $15.00 USD Received 16 Feb 2011; revised 21 Mar 2011; accepted 29 Mar 2011; published 9 May 2011

IDB finally starts to spread out slowly at $z \sim 240$ cm. The peak intensity for the two regimes as a function of the propagation distance is shown in Fig. 3(a).

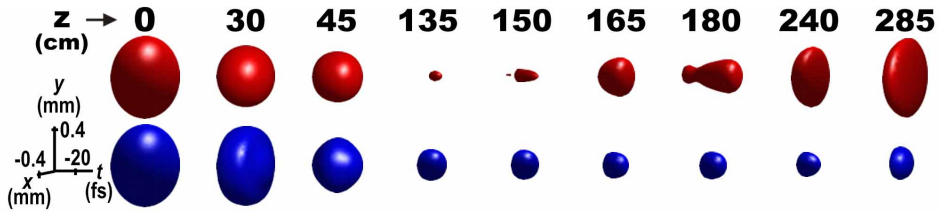

Fig. 2. (Color Online) 3D iso-surface plots of the intensity distributions for the cases of (a) standard filamentation (red iso-surfaces, first row) and (b) IDB formation inside the periodic lattice (blue iso-surfaces, second row), for various propagation distances (Media 1). Isovalue is set to half of the peak intensity at each z position.

In order to investigate the interplay between different physical mechanisms responsible for the IDB formation, we performed numerical experiments by switching off each of the relevant effects, at $z = 150$ cm, where the IDB is already formed. Namely, we considered the effects of dispersion, self-steepening (shock-terms) and the periodic potential. Figure 3(b) shows the radially averaged pulse duration over a 100 μm radius which corresponds to the central cylinder of the lattice. The duration of the IDB remains nearly constant to about 15 fs over 90 cm (continuous curve). When group velocity dispersion (GVD) is switched off at $z = 150$ cm, the IDB with peak power above P_{cr} undergoes self-compression due to the competition between self-steepening and nonlinearity (Kerr focusing and plasma defocusing). This leads to a continuous decrease of the pulse duration [dash-doted curve in Fig. 3(b)] that ultimately becomes shorter than the single cycle limit (not shown here) and results from a well identified singularity of the standard filamentation model in the absence of GVD [30]. The periodic lattice modifies the effective diffraction of the beam and plays a crucial role in its stabilization since the pulse duration increases [dotted curve in Fig. 3(b)] if the lattice is replaced by air. In this case, the beam survives until $z = 170$ cm but then rapidly disperses. Finally the dashed curve depicts the pulse duration if the shock-term is switched off at $z = 150$ cm. The comparison of the dashed and continuous curves shows that the shock-term is essentially limiting dispersion since the pulse broadens in its absence.

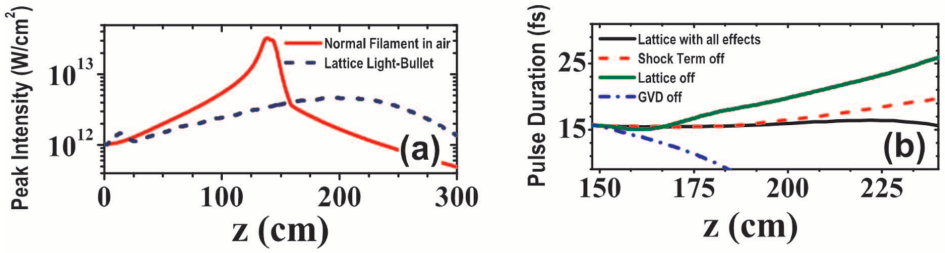

Fig. 3. (Color Online) (a) Peak intensity vs z for a standard filament in air (continuous line) and the IDB (dashed line). (b) Pulse duration (Radially averaged over 100 μm) of the IDB vs propagation distance z when all effects are accounted for (continuous curve) or when a specific effect is switched off at $z = 150$ cm: dotted curve: the lattice is removed; dashed curve: self-steepening is switched off; dash-doted curve: GVD is switched off.

From these numerical experiments, we identified the physical effects that dynamically balance each other to generate an IDB via nonlinear propagation in the periodic potential. Fig-

#142489 - $15.00 USD Received 16 Feb 2011; revised 21 Mar 2011; accepted 29 Mar 2011; published 9 May 2011

ure 4 shows the evolution of typical lengths characterizing these effects, namely the Kerr effect $L_{\mathrm{Kerr}} = (k_0 n_2 I)^{-1}$, diffraction $L_{\mathrm{Diff}} = k_0 R^2/2$, Dispersion $L_{\mathrm{GVD}} = T^2/2k_0''$, MPA $L_{\mathrm{MPA}} = 1/(2\beta_K I^{K-1})$, self-steepening $L_{\mathrm{Shock}} = cT/n_2 I$ and the effect of the lattice $L_{\mathrm{Lat}} = (k_0 \Delta n)^{-1}$. In these expressions, the peak intensity of the pulse I varies as a function of propagation distance, as well as the filament width R and the shortest pulse duration T supported by the pulse spectrum. For standard filamentation [Fig. 4(a)], the main prevailing effect is MPA as indicated by the shortest lengths of all effects over the whole filamentation distance $130 < z < 150$ cm. The Kerr and self steepening effects need centimetric lengths to play a role while diffraction and dispersion need about 10 cm. Thus the filament lives for about 20 L_{MPA} or equivalently one L_{Diff} or L_{Disp}. For the IDB [Fig. 4(b)], the intensity is stabilized by the lattice at a lower level than that reached in the filament, thus the Kerr effect prevails with a typical length in the range 10–15 cm over the whole propagation distance $150 < z < 240$ cm. Two independent equilibria take place in the spatial and temporal dimensions: For the spatial equilibrium, diffraction and the lattice effect with lengths in the range 30-40 cm both compete with the Kerr effect as $1/L_K \sim 1/L_{\mathrm{Diff}} + 1/L_{\mathrm{Lat}}$. For the equilibrium of the pulse profile, self-steepening and dispersion compete with self-phase modulation induced by the Kerr effect as $1/L_K \sim 1/L_{\mathrm{Shock}} + 1/L_{\mathrm{Disp}}$. These two separate equilibria maintain the peak intensity below ionization threshold for a propagation distance of about 10 L_K or 2 L_{Disp}, which is a factor of at least 5 larger than the filamentation length for the same input pulse.

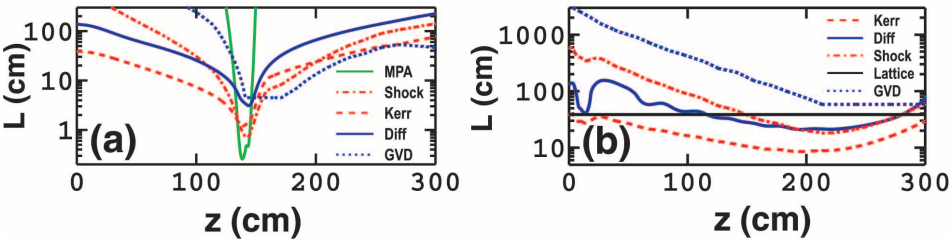

Fig. 4. (Color Online) The smallest lengths characterize the most important physical effects in competition along the propagation axis. (a) Case of a standard filament. (b) Case of an IDB in a periodic lattice.

5. Conclusion

In conclusion, we have shown numerically that filamentation of intense pulses in a radial symmetric periodic potential leads to the generation of intense dynamic bullets. Their intensity is above 10^{12} W/cm^2 and their power is above P_{cr} while they exhibit a quasi-stationary spatiotemporal profile for long propagation distances as a result of the competition of linear and nonlinear effects. In the spatial domain the Kerr self-focusing is mainly balanced by the combined action of the effective lattice diffraction whereas in the temporal domain self-steepening and normal dispersion compete with self-phase modulation. Since the lattice parameters are in a feasible regime for experimental realization (refractive index changes in the order of 10^{-7} and periodicity of $350\,\mu$m), these intense dynamic bullets can be realized in transparent media using permanent or transient refractive index modification induced by high power commercial fs laser sources.

Acknowledgments

This work was supported by the European Union Marie Curie Excellence Grant MULTIRAD MEXT-CT-2006-042683.

#142489 - $15.00 USD Received 16 Feb 2011; revised 21 Mar 2011; accepted 29 Mar 2011; published 9 May 2011